WORCESTER POLYTECHNIC INSTITUTE

Toward Development of Intermediate Temperature Fuel Cells

A Major Qualifying Project:

Submitted to the faculty

Of the

WORCESTER POLYTECHNIC INSTITUTE

In Partial Fulfillment of the requirements for the

Degree of Bachelor of Science

By

Fidelis Wambui

Date: 4/29/2010

Approved by:

Professor Ravindra Datta, Major Advisor

Abstract

The purpose of this project was to develop a better DMFC by reducing methanol crossover and increasing the temperature of the cell. This was done by using a palladium layer on the membrane and a phosphoric acid electrolyte. The palladium (Pd) layer was plated on nickel oxide using electroless plating method. The membrane was then impregnated with H_3PO_4. H_3PO_4 was chosen due to its high conductivity at temperature ranges of up to 200^0C. Although the fuel cell failed to produce current, Open Circuits Voltage was produced when using a NiO membrane impregnated with phosphoric acid. More phosphoric acid needs to be impregnated in the membrane in order to produce higher OCV. However the NiO proved to be a successful support for intermediate temperature fuel cells using H_3PO_4electrolyte.

Contents

Table of Figures

List of Tables

1. Introduction

The purpose of this project was to develop a better direct methanol fuel cell by reducing methanol crossover and increasing the temperature of the cell. This was done by using a palladium layer on the membrane and a phosphoric acid electrolyte. The palladium (Pd) layer was plated on nickel oxide using electroless plating method. The membrane was then impregnated with phosphoric acid. Phosphoric acid was chosen as it has high conductivity at temperature ranges of up to 200^0C. at this high temperature ranges, a fuel cell is less susceptible to carbon monoxide poisoning and other issues as discussed in chapter 2.

The fuel cell using the Pd plated NiO membrane impregnated with phosphoric acid electrolyte was assembled and tested. The results of several testings found that Pd plated NiO was not successful in producing current or voltage in a fuel cell and more phosphoric acid is necessary to produce voltage in a NiO membrane without a Pd layer.

The rest of this chapter will introduce fuel cells, and thermodynamic and kinetic analysis. Other chapters will discuss Goals of the project, methodology used in testing the fuel, results of the experiments and the conclusion and recommendations for future tests.

1.1 Energy Issues

As technological advancements occur, the demand for energy has increased. As people attempt to raise their standards of living using technology such as cars, computers, heating and cooling equipment and leisure tools, their energy use escalates accordingly. Thus as more countries become more industrialized, the energy use globally will exponentially increase and as has been witnessed so far, fossil fuels are decreasing substantially and will no longer be able to support such energy demands.

Figure 1, energy consumption is divided in four major sectors: commercial, residential, industrial and transportation. Commercial sector accounts for stores, offices, schools, hospitals, hotels and other similar buildings. Residential sector are homes, apartments, condos and other similar buildings. Both commercial and residential energy uses consist of heating, cooling and lighting. Transportation sector consists of vehicles that are used in the transporting of people and goods such as trains, buses, cars, boats and others. The industrial sector comprises of manufacturing, agricultural, mining and construction facilities and equipment. In this sector, the equipment used consumes a lot of energy and some facilities operate 24 hours a day and thus use a lot of energy in maintaining HVAC systems and lighting.

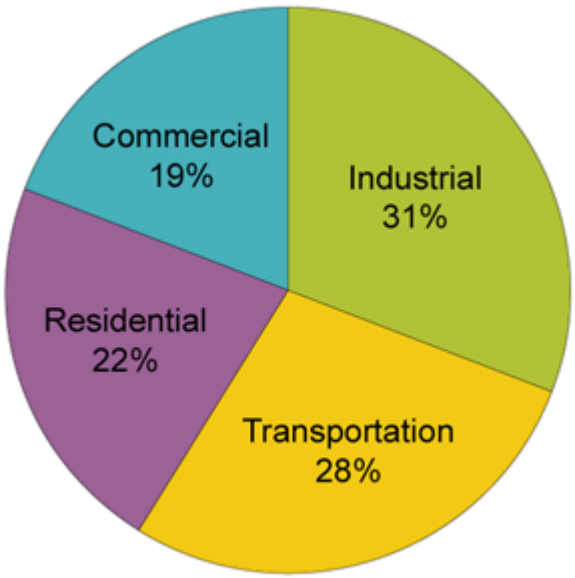

Figure 1: Share of Energy Consumed by Major Sectors of the Economy (2008). (U.S. Energy Information Administration)

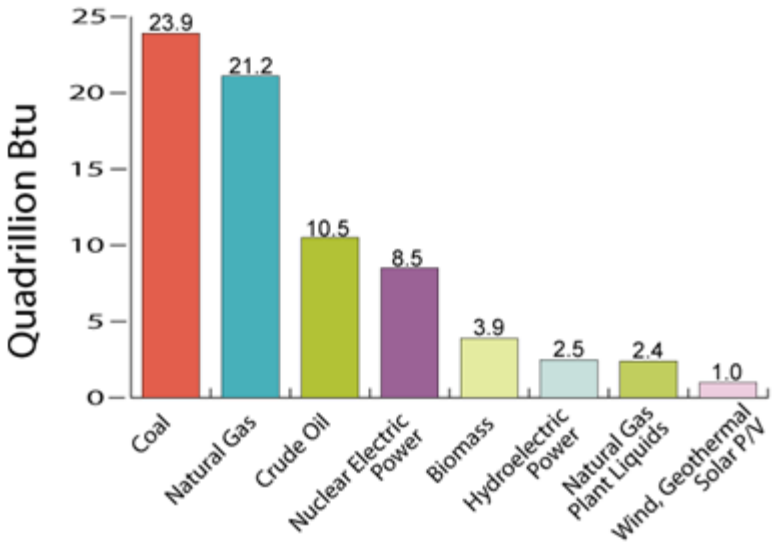

Figure 2: U.S. Primary Energy Production by Major Source (2008) (U.S. Energy Information Administration)

In the U.S, most of the energy produced is from fossil fuels as shown in Figure 2. Renewable sources of energy, such as wind and hydroelectric power, make up about 10%. The increase in technological advances along with the demand for higher standards of leaving has created a strain on energy sources, in particular fossil fuels. As fossil fuel sources continue decreasing, renewable sources will have to be increasingly utilized in order to fulfill the demands.

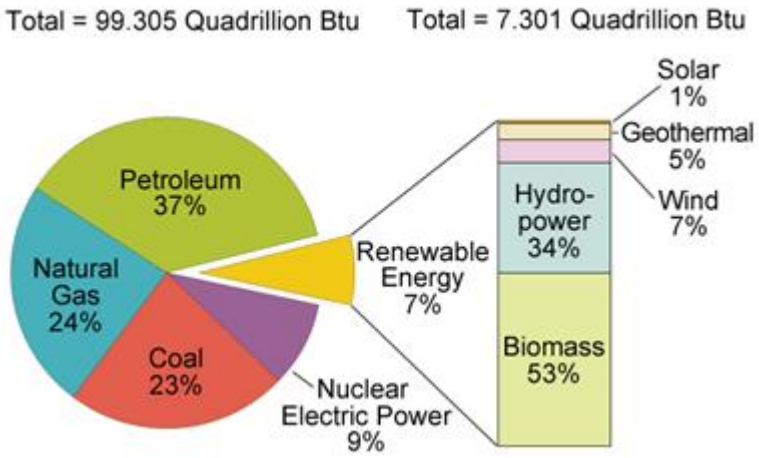

Figure 3: U.S. Energy Consumption by Energy Source (2008) (U.S. Energy Information Administration)

Figure 3 illustrates that petroleum accounts for the largest energy source consumed in the U.S at about 37% while renewable sources only account for about 7%. One of the major issues, besides the continue decreasing of fossil fuels, is the environmental damage associated with petroleum, coal and natural gas.

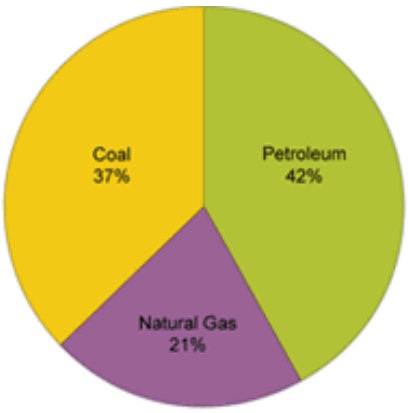

Figure 4: Resulting Carbon Monoxide Emissions from fossil fuel consumption (2008) (U.S. Energy Information Administration)

Figure 4 shows the effects of using fossil fuels on the production of carbon monoxide. The result of using fossil fuels as approximately 84% of the energy source in the U.S is that approximately 99% of the carbon dioxide emitted is from these fuels' consumption. Carbon dioxide emissions make up 81% of the greenhouse gases emitted in the U.S that are caused by humans and not by natural causes such as plants and volcanoes. Carbon dioxide and other greenhouse gases are responsible for the changes in climate globally, melting of polar ice caps and other global warming effects.

1.2 Fuel Cells

The energy and environmental issues currently being faced globally have made a new energy alternative a necessity. Renewable energy sources have been integrated into some European countries, some of which plan on running fully on renewable energy in a few decades. Fuel cells have emerged as another technology in the quest for replacing fossil fuels and reversing the effects of greenhouse gases. Fuel cells promise clean and efficient power generation.

A fuel cell is an electrochemical device that combines hydrogen fuel and oxygen from the air to produce electricity, heat and water. Using fuel cells is extremely efficient as the fuel is converted directly to electricity and less pollution is produced as the fuel cells operate without combustion such as is common in converting fossil fuels into usable fuel and electricity. (Larmine and Dicks)

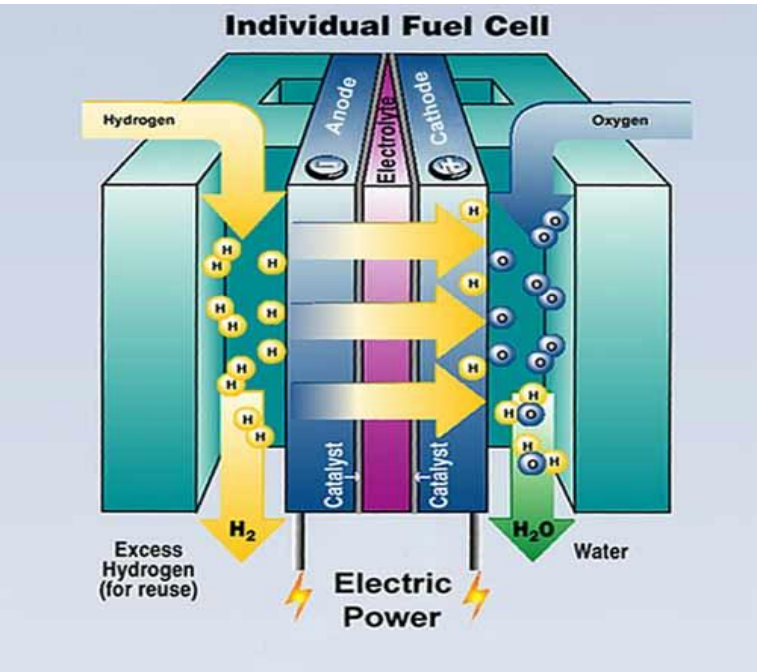

Figure 5: Composition of an individual fuel cell

As shown in Figure 5, "the fuel cell is composed of an anode, which is a negative electrode that provides electrons, an electrolyte in the center and a cathode (a positive electrode that accepts electrons)" (www.utcpower.com). The anode contains a platinum catalyst that aids in the separation of the gas into protons (hydrogen ions) and electrons as hydrogen flows into the fuel cell. The electrolyte in the center allows only protons to pass through to the cathode side, which forces the electrons to flow through an external circuit in the form of an electric current that can power an electric load. Another platinum catalyst in the cathode aids in the combination of the oxygen, protons, and electrons to produce pure water and heat. In order to increase voltage, fuel cells can be combined into fuel cell stacks, which

determine the total voltage. The surface area of each cell determines the total current. To determine the electrical power generated, multiply the voltage by the current (P=V*I).

In the delivery of hydrogen, fuel cell systems use a fuel reformer, which is a "fuel processor that extracts hydrogen from hydrocarbons such as natural gas if methane gas produced in wastewater treatment plants" (www.utcpower.com). The current produced is direct current (D/C) and then a power inverter is used to change the electricity to alternating current (A/C), which is the electrical standard for most uses. If the hydrogen is available as a direct resource, neither the reformer nor the inverter is necessary.

1.2.1 Types of Fuel Cells

There are several types of fuel cells and they are primarily classified by the kinds of electrolytes they employ. Polymer electron or proton exchange membrane fuel cells (PEMFC) and direct methanol fuel cells (DMFC) are explained in this section as DMFC is similar to PEMFC and the DMFC tested in the experiments used only hydrogen not methanol as PEMFC does.

1.2.1.1 PEMFC

Polymer electrolyte membrane fuel cells, also known as proton exchange membrane fuel cells, are low temperature fuel cells operating at room temperature to 100^{0}C and pressures of 1-3 atm. As shown by Figure 6, in a PEM fuel cell hydrogen is oxidized on the negatively charged electrode (anode) while oxygen is reduced in the positively charged electrode (cathode). The oxygen reacts with the protons and electrons on the cathode producing heat and water. The protons are transported from the anode to the

cathode through the electrolyte membrane and the electrons are carried over an external circuit load.

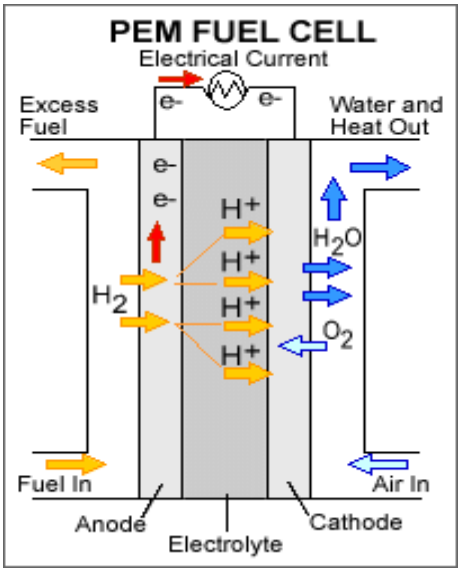

Figure 6: Proton exchange membrane (PEM) Fuel Cell (U.S. Department of Energy)

The reactions that take place in a PEMFC are:

Anode: $H_2 \leftrightarrow 2H^+ + 2e^-$

Cathode: $\frac{1}{2}O_2 + 2H^+ + 2e^- \leftrightarrow H_2O$

Overall Reaction: $H_2 + \frac{1}{2}O_2 \leftrightarrow H_2O$

The most common electrolyte used is Nafion (perflourosulfonic acid membrane) made by DuPont and the most common anode catalyst is Platinum at a thickness of 10-30 micrometers.

There are several advantages of this fuel cell that make it quite usable in vehicles. It can start quickly as it operates at low temperatures, which aids in starting vehicles in the mornings or during cold seasons. It has a high power density, which means that it produces a high amount of power relative to its size. This makes it a great fuel cell for vehicle or mobile phone applications as it can be lightweight and compact. Thus the main applications of PEM fuel cells are in vehicles, stationary and portable uses such as mobile phones.

1.2.1.2 DEMFC

The direct methanol fuel cell (DMFC) was developed as a solution to the problems in supplying hydrogen to fuel cells. As its name implies, the direct methanol fuel cell uses methanol directly as a fuel. The methanol flows through the anode as fuel and is then broken down into protons, electrons and water. The protons flow through to the cathode while the electrons flow around the electrolyte and form an electrical current. In the anode, the liquid methanol and water react and form carbon dioxide, protons and electrolytes. At the cathode, the electrons and protons react with oxygen to form water. This fuel cell operates at room temperature to 100 degrees Celsius and has an efficiency of about 40 percent, which is standard for most fuel cells. (Larmine and Dicks)

There are some great advantages of using methanol as a fuel rather than hydrogen. Methanol has a higher net energy density than other fuel options for the fuel cell. Hydrogen offers lower energy per volume compared to methanol which offers more than four times. The DMFC system is easier to use and very quick to refill as well as lower in weight. However, the biggest advantage to using methanol directly as the fuel rather than hydrogen is that methanol is widely available and easily reformed from biomass or gasoline.

If fuel cells are to become a widely viable and commercial product with hydrogen as the main fuel, a hydrogen infrastructure will have to be developed to support it. This will include not only production but also storage, transportation and dispensing of the hydrogen. Although there are several methods of producing hydrogen and many governments worldwide have set high production goals for the next few years, most production methods are extremely costly. Steam reforming of natural gas is rising as the least expensive method for production. This method uses fossil fuels, which are on a continuous decrease and also produce carbon monoxide in the process. And as mentioned before, storage and transporting the hydrogen produced is still an issue. One of the common technologies of storing

hydrogen is in large pressurized tanks. However most of these tanks are extremely heavy and would be inconvenient in the use of fuel cells as they cannot be easily stored in vehicles that use fuel cells and other similar applications. Another method of storing hydrogen would in as a liquid but this method is also very expensive as large amounts of energy are necessary in the production of hydrogen and in maintaining the hydrogen at the proper low temperatures. In dispersing the necessary hydrogen for use in fuel cells, especially in vehicles, refueling stations similar to those used for gasoline would be necessary to make the use of hydrogen fuel cell vehicles easier and more accepted. However, storage and transportation issues as well as production cost problems would have to be solved. Thus, using methanol as a fuel solves some of these issues as the storage and production of methanol is currently less expensive than that of hydrogen. (Spiegel)

However, while methanol as a fuel is extremely advantageous, there are several reasons that keep the technology form being widely adapted. One of the major problems is that of the fuel crossover through the electrolyte to the cathode. As the membrane used in the DMFC is a proton exchange membrane (PEM), it absorbs the methanol and mixes with the water, which flows into the cathode from the electrolyte. This greatly affects the open circuit voltage (OCV) as well as all other circuits and the slow oxidation process in the anode while also wasting fuel. The second problem is the slow oxidation of methanol in the anode. This means that the fuel cell has lower power for a given size and large overpotentials are necessary for high power output. Another issue is the poisoning of the electrode by the hydrocarbon intermediate species produced during the oxidation of methanol. (Spiegel)

To resolve these issues, there are several things that must be accomplished. The membrane electrode assembly (MEA) must be made more durable, the membranes' selectivity must be improved to reduce the crossover rate and the anode must be improved for better methanol oxidation catalysis. In this paper, I will explore a possible solution to the cross-over of methanol in the electrolyte to the cathode.

1.2.2 Thermodynamic and Kinetic Analysis

In understanding the science and technology behind direct methanol fuel cells, a thermodynamic and kinetic analysis was performed. This included determining the regions of feasibility for the reactions, the relationship between current densities and electrode potential, polarization curves and the effect of methanol crossover on the current. The effect of temperature is analyzed in the next section entitled "Intermediate Temperature Fuel Cells."

The reactions that occur in a DMFC are as follows:

Anode: $CH_3OH + H_2O \leftrightarrow CO_2 + 6H^+ + 6e^-$

Cathode: $\frac{3}{2} O_2 + 6H^+ + 6e^- \leftrightarrow 3\ H_2O$

Overall Reaction: $\frac{3}{2} O_2 + CH_3OH \leftrightarrow CO_2 + 3\ H_2O$

The changes in enthalpy, entropy and Gibbs free energy were calculated for each reaction. It was assumed that the water was liquid as was the methanol since the reaction occurs below 100 degrees Celsius. The reactions were assumed to occur at standard conditions of 298K and 1 atm. The equations used in calculating the changes in enthalpy, entropy and Gibbs free energy are illustrated in Appendix 1, equations 1, 2 and 3. Using the calculated values for the change in Gibbs free energy, the standard equilibrium potential was also determined for the anode and cathode. Table 1 shows the results of the calculations.

Table 1: Anode, Cathode and Overall Reactions Thermodynamics

P	$\Delta G^0_{p,\Phi=0}$ (J/mol)	ΔH^0_p (J/mol)	ΔS^0_p (J/mol*K)	$\Phi^0_{0,p}$ (V)
Anode	5350	93620	296	$9.24*10^{-3}$
Cathode	-711420	-857490	-490	1.229
Overall Reaction (OR)	-706070	-763870	-193.96	

1.2.2.1 Regions of Feasibility

The region of feasibility describes the temperatures and equilibrium potential ranges in which the dmfc reactions are thermodynamically possible to occur. To determine this region, the changes in entropy, enthalpy and Gibbs free energy were used in the equations for the equilibrium constants shown below, Eq. 1 and 2.

$$K_\rho = \exp\left(-\frac{\Delta G^\circ_{\rho,\Phi=0}}{RT}\right)\exp\left(\frac{\nu_{\rho e^-} F\Phi}{RT}\right) = \left\{K_{\rho,\Phi=0}\right\}\exp\left(\frac{\nu_{\rho e^-} F\Phi}{RT}\right) \qquad \text{Eq. (1)}$$

$$K_{p,\Phi=0} = \exp\left(\frac{\Delta S^0_p}{R}\right) * \exp\left(-\frac{\Delta H^0_p}{RT}\right) \qquad \text{Eq. (2)}$$

These two equations simply, when solved for In K_p, to show the dependence of the equilibrium constant on temperature and potential:

$$In\ K_p = \left(\frac{\Delta S^0_p}{R}\right) - \left(\frac{\Delta H^0_p}{RT}\right) + \frac{\nu_{p\,e} - F*\Phi}{RT} \qquad \text{Eq. (3)}$$

When K_p=1, the potential is determined and when the potential is set to zero, the equilibrium potential is determined. These values are determined for both the cathode and the anode. This gives the parameters for the temperature-phase diagram as shown in table 2. These parameters are plotted as illustrated in Figure 7 and 8.

Table 2: Perimeters for the temperature-phase diagram

Anode		**Cathode**	
T(K)	Φ (V)	T(K)	Φ (V)
0	0.000162	0	1.481184
316.2838	0	1749.98	0

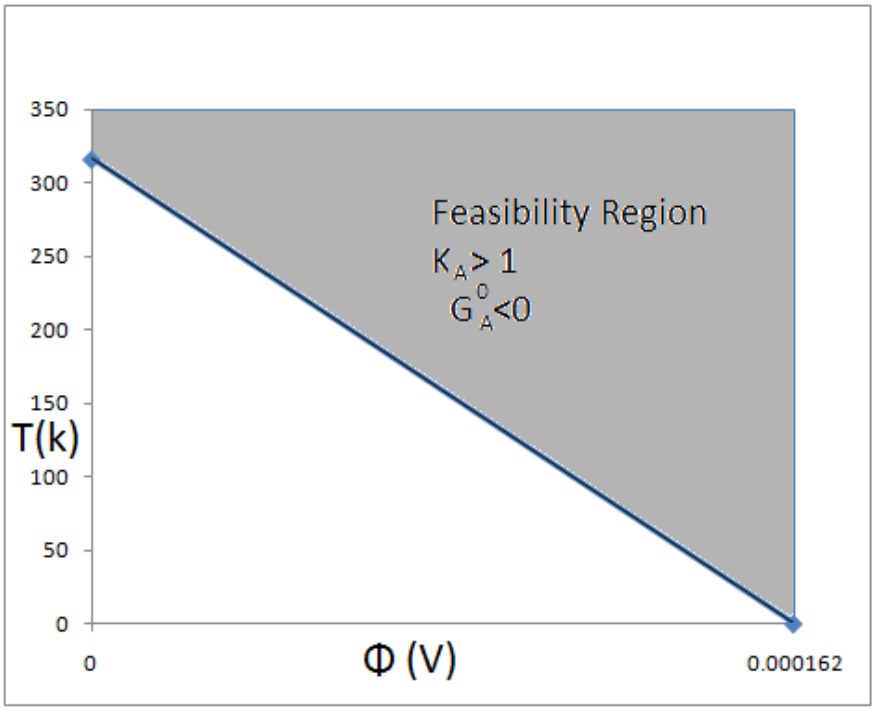

Figure 7: Region of Feasibility for the Anode

Figure 7 illustrates that at the normal operating temperature of DMFCS, 80 degrees Celsius (353 K), the anode reaction is favorable thermodynamically. Although this reaction has a slow kinetic rate, which causes some disadvantages in the DMFC as discussed earlier in the chapter, it does not require any potential to occur.

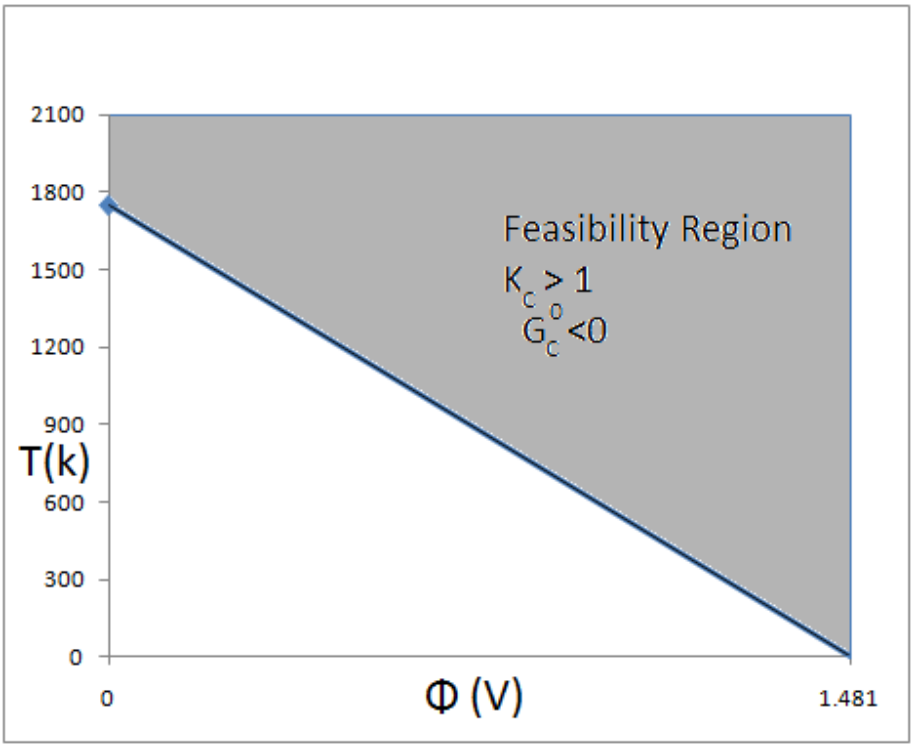

Figure 8: Region of Feasibility for the Cathode

However, the cathode reaction requires approximately 1.2 V of potential in order to be thermodynamically favorable as illustrated in Figure 8.

1.2.2.2 Methanol Crossover

One of the biggest issues in DMFCs is the crossover of methanol from the anode to the cathode through the electrolyte. This issue is caused by the nafion electrolyte's permeability to methanol fuel. This issue greatly affects the open current voltage. Decreasing the methanol feed reduces the crossover rate. However, higher methanol feeds produce larger power densities. Increasing the current decreases the crossover as more methanol fuel is consumed at the anode rather than crossing over into the cathode. (Ramya and Dhathathreyan)

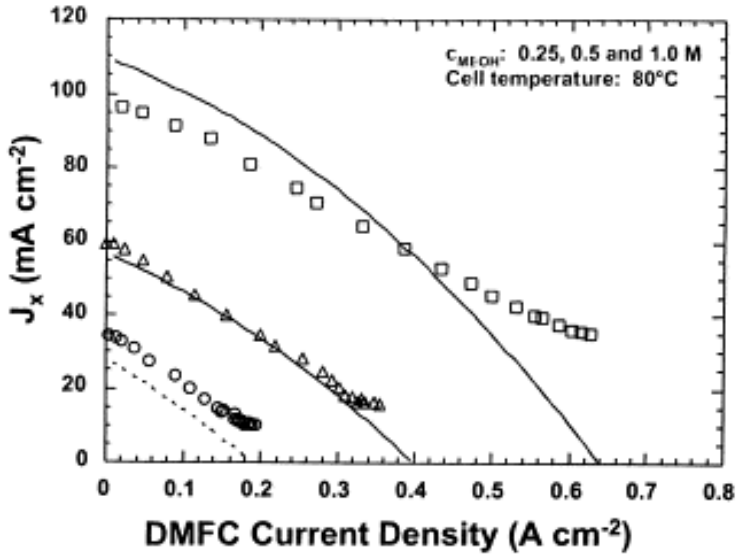

Figure 9: Rate of methanol crossover current (J_x) as a function of DMFC current density using three methanol feed concentrations (Ren and Zelery, 2000)

Figure 9 illustrates that the rate of methanol crossover current decreases as the current density increases. As the feed rate is lowered from 1M methanol to 0.5 M and 0.25M the crossover current decreases. As noted before, lowering the methanol feed rate decreases the crossover as there is little fuel available to crossover to the cathode from the anode. As the limiting current density is approached, the crossover current approaches zero. However, this may not apply to real fuel cells and may only work in theory. In real applications, as found in experiments, even if the limiting current is approached there is always some crossover current in nafion electrolytes.

1.2.2.3 Polarization Curves

To determine the relationship between the cell voltage and the current density and plot the polarization curves, the Butler-Volmer Equation was used. Using the parameters shown in Table 3 below, MathCAD was used to solve for the cathode and anode potential. The calculations are shown in Appendix 1.

Table 3: Parameters for DMFC operating at 353 K (80^{0}C) and 1 atm

Component	Parameter	Value	Source
Anode	α_A	0.239	Wang & Wang, 2003
	ν_{Ae^-}	6	Assumed
	λ_{MA}	150 cm^2 Pt/ cm^2 MEA	Assumed
	i_{AL}	41.4 A/cm^2 MEA	Scot et al.
	i_{A0}	1.4145 A/cm^2 MEA	Wang & Wang, 2003
cathode	α_c	0.5	Garcia et.al
	ν_{ce^-}	-2	Assumed
	λ_{MC}	150 cm^2 Pt/cm^2 MEA	Assumed
	i_{CL}	1.5 A/cm^2 MEA	Scot et al.
	i_{C0}	0.00063 A/cm^2 MEA	Wang & Wang, 2003
Electrolyte	L_{EL}	125 µmeters	Assumed
	σ_{EL}	0.123 S/cm	Yang and Liang, 2009

To plot Voltage as a function of current, the following equation was used

$$V = V_0 - \eta_A - \eta_C - \eta_{EL} - \eta_L$$

η_A and η_C were determined using MathCAD. While η_{EL} and η_L were determined using the equations shown below.

$$\eta_{EL} = \frac{iL_{EL}}{\sigma_e}$$

$$\eta_L = iR_1 = 0$$

The resistance was assumed to be zero. The data was plotted as shown in Figure 10.

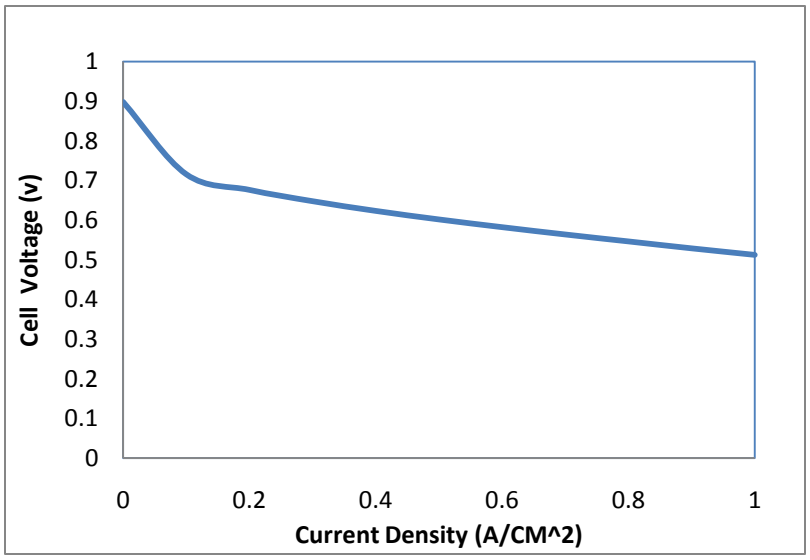

Figure 10: Polarization curve for DMFC at 353K and 1 atm

The curve in Figure 10 illustrates that an increase in current density results in a decrease in the cell voltage. The rate of decrease in voltage levels of after around 0.2 A/cm^2. The initial drop in voltage is due to the large overpotential necessary when the current is below 0.2 A/cm^2. While an increase in current density decreases the overpotential, an increase in temperature also has the same effect. This is discussed in the intermediate fuel cell temperature section.

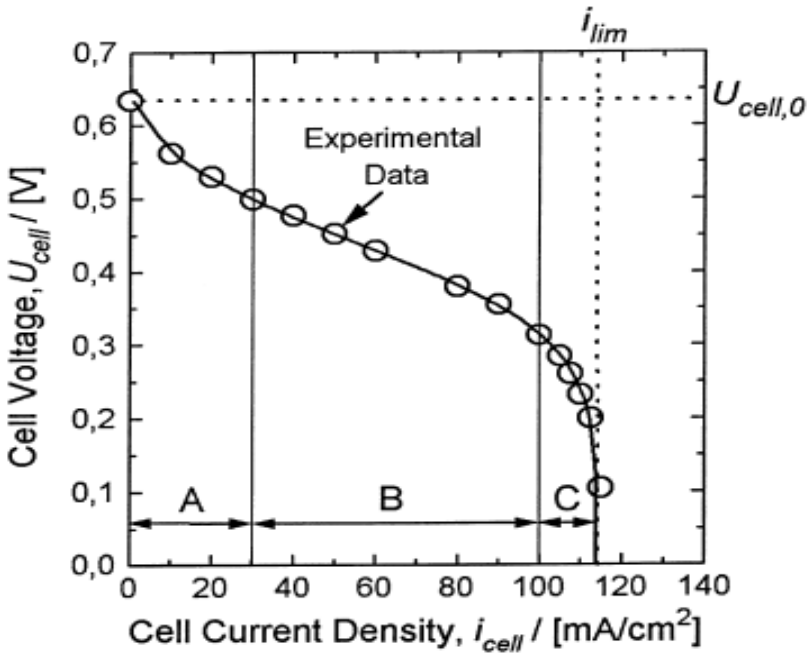

Figure 11: Polarization curve for DMFC at 70 degrees Celsius and 1 atm, Sundmacher et al., 2001

Figure 11 illustrates a polarization curve from literature. Just as the calculated data shows, there is a large drop in voltage at the beginning due to the large overpotential necessary to run the fuel cell at low current density. This is because the methanol oxidation reaction occurs in the region marked A. This region requires more overpotential as the kinetic rates are much slower for this reaction in DMFCs. At region C, the cell approaches the limiting current density which is where the voltage of the cell approaches zero. Other models in literature show that the limiting current density increases as the methanol feed increases. The increase in methanol increases the fuel available for the cell, and decreases the effects of methanol crossover. The limiting current density is the limiting factor in DMFCs. (Sundmacher, Schultz and Scott). Compared to Figure 11, the calculated data in Figure 10 overpredicts the performance. The calculated data did not take into consideration the effects of resistance, especially ohmic resistance on voltage. Figure 10 data may have also used different methanol feed concentration than that used in Figure 11, which would also affect the potential of the cell.

1.2.2.4 Power Density and Efficiency

To determine the effectiveness of fuel cells, the power density must be analyzed. The power of a fuel cell is proportional to the current density and voltage as shown in the equation below.

$P = i * V$

The power density for DMFC at 353K and 1 atm is shown in Figure 12.

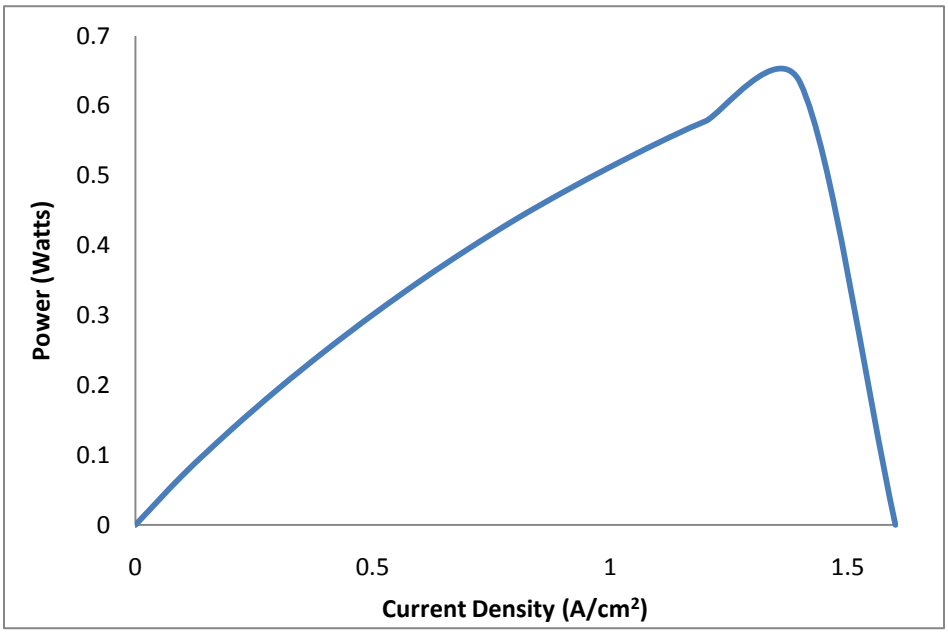

Figure 12: Power density of DMFC at 353K and 1 atm

The power density plotted in Figure 12 shows that as the current density increases, the power density increases. Although this plot does not indicate so, at a certain current density the power density starts decreasing and mirrors the beginning of the curve forming an n-shaped curve. This is due to the dependence of power on voltage as well as current. At the beginning as current increases, the power also increases but as voltage continues to decrease with the increase in current, so does the power density.

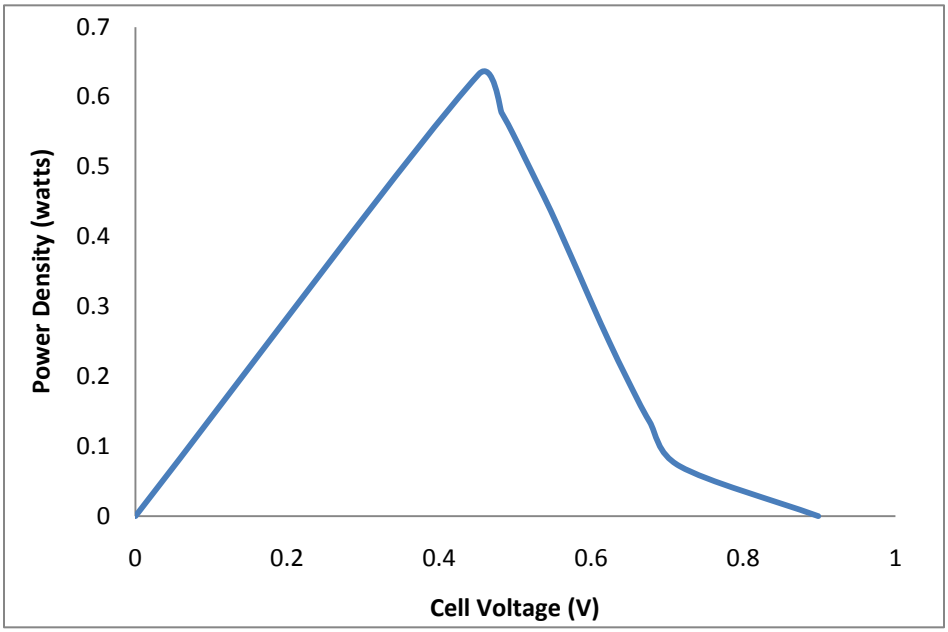

Figure 13: Power density as a function of cell voltage for DMFC at 353K and 1 atm

Figure 13 shows a similar relation of power density and cell voltage as that of power and current. This illustrates as mentioned before that power density increases with voltage before decreasing as the effects of current increase. This means that at the maximum power density shown on the graph is not the best power to operate a fuel cell as it may produce a low voltage. Thus most fuel cells do not operate at optimum power density but rather at the power density that produces both current and voltage well.

To determine the efficiency of the cell, the equation below was used.

$$\varepsilon = \frac{V_{cell}}{V_{max}}$$

The maximum voltage was determined to be 1.32 V. The efficiency was plotted and is illustrated in Figure 14.

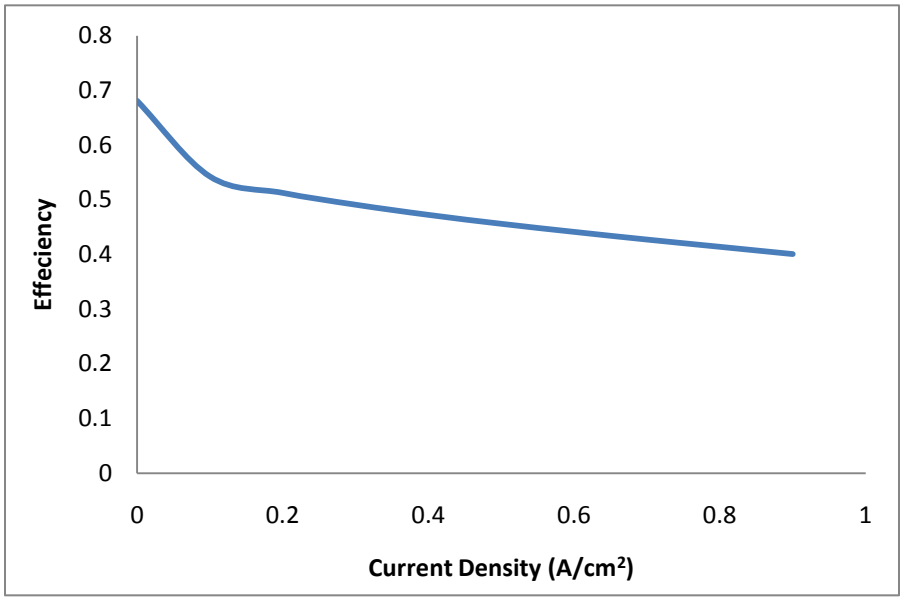

Figure 14: Efficiency of DMFC as a function of Current Density at 353 K and 1 atm

As Figure 14 shows, the plot of efficiency with relation to Current is similar to that of cell voltage and current. This is due to the linear relationship of efficiency and current voltage. The maximum efficiency is 68%, which occurs when the cell potential is very high. Although the highest power density is not produced at the highest cell voltage, the system is extremely efficient at that level. However, DMFCs operate at 40%. These conditions are continuously evaluated in order to improve efficiency of the cell.

2. Goals and Objectives

The goal of the project was to improve the performance of DMFC by reducing the methanol crossover as well as increasing the temperature. The objective of the project is to investigate electroless-deposited palladium membrane direct methanol fuel cells and the use of porous ceramic as the membrane and phosphoric acid or potassium hydroxide as the electrolyte. As discussed in the previous chapter, methanol crossover highly diminishes the voltage of the cell and decreases the available stack fuel. The cathode polarization is also increased, which positively affects the voltage in the cell. Increasing the temperature would increase the kinetic rates of the methanol oxidation reaction and reduce the production of the hydrocarbon intermediate species that poison the fuel cell.

A thin (1-5 micrometer) layer of palladium was to be plated on the membrane. The palladium layer plated will occur at a rate of approximately 1.2 mg/cm^2/µm thickness as determined by the density of the palladium. To plate 5µm thick membrane, approximately 5 palladium loadings would have to be done which would result in 6 µm thickness. This is similar to a conventional DMFC anode using platinum. The membrane was then to be impregnated with either phosphoric acid or molten potassium hydroxide. In assembling the fuel cell, the impregnated membrane was sandwiched between two carbon cloth electrodes with platinum electrocatalyst. The ceramic layer acts as a support for the electrolyte.

The resulting DMFC should have a better performance as the methanol crossover is reduced, the cathode polarization and the positive effects of the increase in temperature. The increase in temperature should reduce the carbon monoxide poisoning of the anode due to the intermediate species formed during the slow methanol oxidation process. This will decrease the polarization in the anode. However, a small polarization is expected due to the hydrogen transport through the palladium layer. The high permeability of hydrogen through palladium should reduce this polarization and make it minimal.

The DMFC would be assembled as described above and tested for voltage and current. A successful DMFC should produce high voltage and current, and have little methanol crossover. It should also operate at higher temperature ranges of 150-200^{0}C. This will prove that the ceramic layer support along with the phosphoric acid electrolyte produce a better DMFC than the conventional one available currently.

The current fuel cell technology operates at temperatures between the ranges of room temperature to 200 degrees Celsius (low temperatures) and 500 to 1000 degrees Celsius (high temperatures). However, there has not been much development in the intermediate temperature ranges between 200 to 500 degrees Celsius. Thus more research is now going into intermediate temperature fuel cells that operate at these ranges.

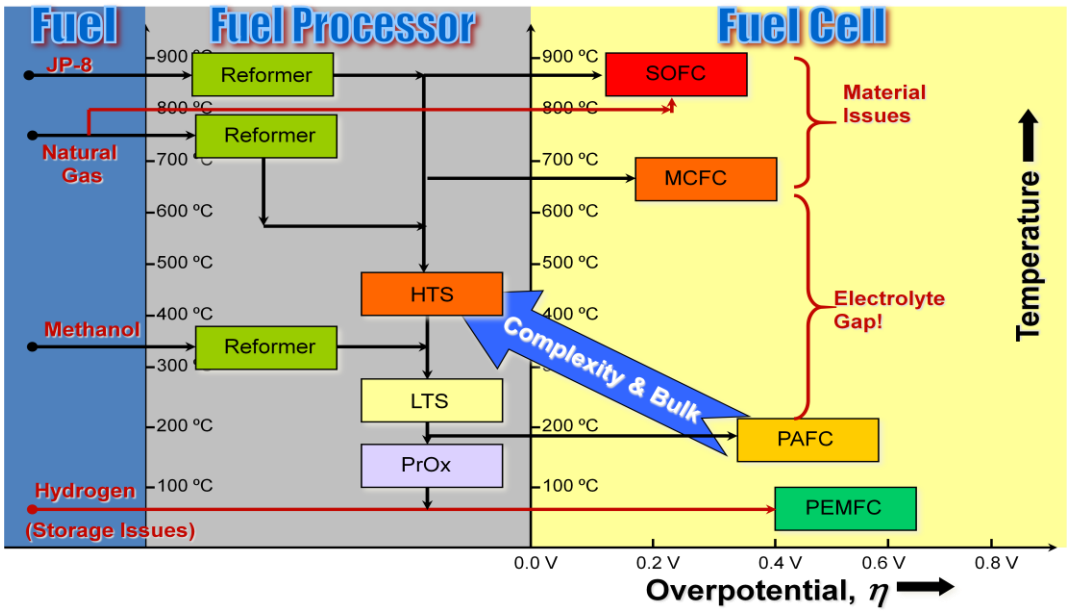

Figure 15: overall fuel cell system including reformer of low and high temperature fuel cells

Figure 15 shows overall fuel cell systems including the reforming of the fuel into hydrogen. As Figure 15 shows, there are several different types of fuel cells that operate at different temperatures. As noted before, there are no fuel cells that operate at the intermediate temperatures. While there are several

issues to increasing the temperature such as not having enough electrolytes or material support, there are also several advantages to increasing the temperature. The major advantage in raising the temperature is that the kinetic rates of the reactions that occur within the fuel cell will be increased. As temperature rises so do the kinetic rates. One major issue in direct methanol fuel cells is the slow oxidation of methanol in the anode. With the increase in temperature, this reaction will occur much faster and the intermediate species formed will no longer be such an issue. Another advantage to increasing the temperature is that more fuel options will become available rather than suing hydrogen alone. This will make fuel cells more viable in commercial and everyday use, especially in vehicles and other applications. The other advantage of higher temperatures is the use of different electrolytes from Nafion. Nafion is an expensive electrolyte and the increase in temperatures will open the possibility of other cheaper electrolytes such as phosphoric acid and molten potassium hydroxide. These and other reasons make increasing temperature a very important goal in new fuel cell technology.

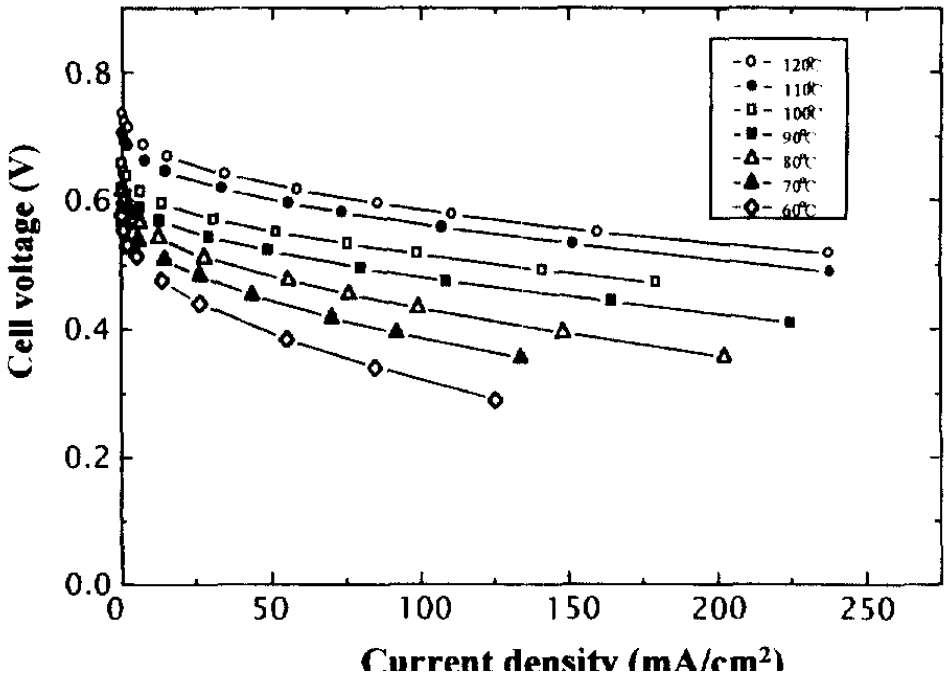

Figure 16: Characterization of DMFC single cell at various Temperatures, Jung et al. 1998

Figure 16 shows the effect of temperature on the cell voltage of DMFC. As discussed in this section, the cell operates better at higher temperatures. As the temperature increases, there is less resistance and polarization increases, thus increasing the performance of the cell.

However, as mentioned before there are several issues in raising the temperature of fuel cells. Some of the major issues are the lack of material support and the lack of electrolytes. While nickel, stainless steel and other supports have been tested for low temperature and yttria stabilized zirconia (YSZ) and molten carbonates have been tested as electrolytes for high temperatures, there is very little for intermediate temperatures. Currently phosphoric acid, which was used in the experiments detailed in this paper, and other acids are being investigated as possible electrolytes for intermediate temperature fuel cells. Phosphoric acid is conductive at temperature ranges above 150 degrees Celsius which makes them an ideal starting point for research. (Bagotsky)

3. Methodology

In order to have a working fuel cell to test, several actions had to be completed. The most important step was making the membrane electrode assembly (MEA), which includes plating palladium on Nickel Oxide and treating it with phosphoric acid as the electrolyte.

3.1 Palladium Electroless Plating

Nickel Oxide metal was plated with palladium using the electroless plating process. A piece of 4 cm by 4 cm Nickel was first cleaned by sonicating it in water for 15 minutes and then sonicating it in acetone for 15 minutes. It was then put in a 990^0C oven for three hours in order to convert it into Nickel Oxide. The nickel oxide was then placed in a 120^0C oven overnight. The next day, the nickel oxide was coated with clear nail polish with a non-coated center of 2.25 cm by 2.25 cm length on one side and a lightly coated portion of the same size on the other side. The non-coated center is the part that would be plated with

palladium as it is the membrane. It was dipped in water for five minutes, followed by one minute in 1 M HCL solution and then put back in the water while preparations of the activation solutions took place. In order to plate the palladium using the electroless plating process, $PdCl_2$, 0.01 M HCL, 1 M H_2NNH_2 and plating solutions were all made previously. $SnCl_2$ solution had to be made fresh each day it was being used to avoid degradation of the solution. The preparation steps of these solutions are in the appendix.

The sensitization and activation of Nickel Oxide took several steps. First, the nickel oxide was then placed in the $SnCl_2$ solution for five minutes, followed by two minutes in water and then three minutes in fresh DI water. The nickel oxide was next dipped in $PdCl_2$ solution for five minutes followed by two minutes in 0.01 M HCL solution and then three minutes in water. The process was then repeated 5 times. To make the process a bit easier, several 100 ml beakers were used. Each of them was labeled according to the solution used: $SnCl_2$, Water 1, Water2, $PdCl_2$, 0.01M HCL and Water after 0.01 M HCL. The activated nickel oxide was then stored in 120^0C oven for an hour.

Before plating the nickel oxide, it was placed in water for five minutes, followed by one minute in 1 M HCL solution. Approximately 70 ml of the plating solution was mixed with 0.80 ml of 1 M H_2NNH_2 solution. The Nickel Oxide was put in the solution before being placed in a 60^0C bath for approximately 90 minutes. After 90 minutes, the nickel oxide was placed in water that was also in the 60^0C bath while a new solution was being mixed. It was then placed in the new plating solution in 60^0C bath for another 90 minutes. This process was done three times to ensure plating of approximately 5 micrometers palladium. The palladium plated nickel oxide was then placed in 120^0C oven overnight to dry. The calculations for determining the thickness of the palladium layer are in appendix 1.

To determine if palladium electroless plating produced a dense layer that was not permeable to other gases besides hydrogen, porous stainless steel (PSS) in a cylindrical shape was plated similar to the method of plating nickel oxide. Before plating, the porous stainless steel was tested using a digital

bubble flow meter to measure the permeability. Gas was pumped at 28.9 PSIG through a tube in which the PSS was tightly enclosed. The permeability was measured by determining how much gas flowed through the PSS by attaching it to the bubble flow meter. The meter determined the capacity by the rising of the bubbles in the flow meter. Before plating, the PSS had a permeability rate of 92.9 ml/min. However after plating, the palladium layer prevented all of the gas from diffusing through as the layer was dense.

3.2 Electrolyte

The electrolyte used for the fuel cell tests was phosphoric acid. To determine if phosphoric acid or molten potassium hydroxide were adequate as electrolytes while using Nickel Oxide support, they were both tested. Nickel Oxide was placed in two beakers each containing one of the electrolyte candidates. The molten potassium hydroxide was made by heating solid potassium hydroxide at 2500C for an hour. The Nickel Oxide was weighed then placed in the potassium hydroxide at this temperature to keep it molten overnight. It was then weighed to determine if there was any weight change. A different Nickel oxide piece was also placed in the phosphoric acid but at room temperature. The weight changes were not extremely significant. Both pieces had a weight gain of one percent in phosphoric acid and 0.6% in molten potassium hydroxide. As it is necessary for the electrolyte to be absorbed into the membrane, the phosphoric acid, which had the most increase in weight, was chosen as the membrane.

A piece of nickel oxide plated with palladium was weighed. Drops of phosphoric acid were placed on the palladium coated piece of nickel oxide for an hour as they were absorbed. The nickel oxide was then put in a beaker of phosphoric acid and placed in a 1000C oven for an hour to ensure maximum absorption. The temperature was then dropped down to room temperature before being taken up again to 1400C for an hour to dry. After drying, the piece was stored in a 400C oven overnight to ensure it was dry. Before weighing to determine if any change in weight, the piece was wiped with a Kimwipe to make sure

there was no film of phosphoric acid on the top layer. To determine how much phosphoric acid was impregnated into the NiO, the calculations are in appendix 1.

3.3 Testing the Fuel Cell

The Nickel oxide plated with palladium and coated with phosphoric acid along with the anode and cathode catalyst make up the Membrane Electrode Assembly (MEA). The first test used a nickel catalyst and the second test of the fuel cell used a carbon cloth with platinum catalyst.

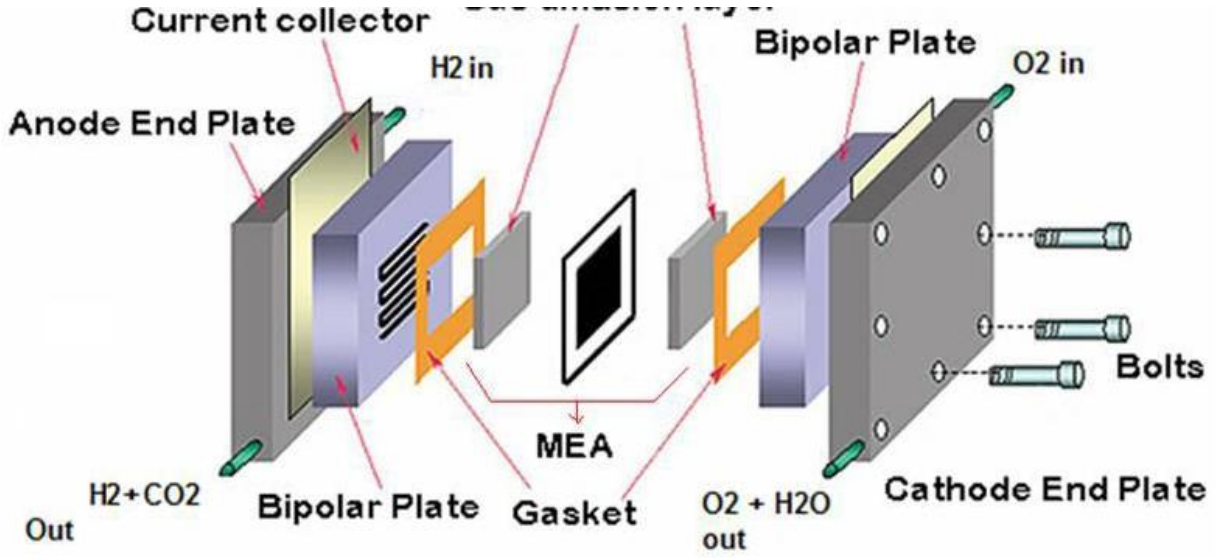

Figure 17: Assembly of Fuel Cell (Gleason, Jensen and Painuly)

The fuel cell was assembled by first setting a thin layer of silicon followed by the gasket and finally another silicon layer. In the gasket contained the NiO with catalyst layer of 2.25cm by 2.25 cm size on both sides of the NiO as illustrated in Figure 17. To make sure that hydrogen flowed through the fuel cell from the anode to the cathode, the fuel supply was turned on and beakers of water were put at the two ends and the appearance of bubbles in the water would be an indication of the flow of gas. The whole machine was then turned on and the current and voltage produced by the fuel cell were monitored. The

temperature was raised from room temperature to 220^0C with more attention paid to temperatures in the range of 150-200^0C as phosphoric acid is more conductive at those ranges.

The test was repeated three times, the first two with different catalysts and the third time with no palladium plating on the nickel oxide. To make that there was enough phosphoric acid electrolyte, a few drops were brushed on the catalysts layers. The fuel cell was tested with hydrogen rather than methanol to first ensure that it worked well. If successful, the tests would be repeated using methanol as fuel.

4. Results and Discussion

Nickel Oxide (NiO) was plated with palladium using the electroless plating process. This process was proved very successful. There were no cracks in palladium layer, and the thickness of the layer was easily controlled as it was dependent on the number of times the NiO was plated. The deposition of the phosphoric acid electrolyte was also successful. However, the electrolyte deposited was very little, with the largest deposition being 0.52% while the lowest was 0.027%. This may have caused some of the issues with the fuel cell current production as more electrolyte was necessary. The use of acrylic nail polish to prevent palladium plating on areas that were not necessary worked. However, the nail polish affects the plating solution as grey precipitation was present in the solution. After plating several times, this precipitation stopped forming but it may have affected NiO. More experiments need to be done to determining whether any negative consequences occurred. There was also precipitation during plating sometimes even without the use of the nail polish. This was usually caused by impurities in the beaker used and the precipitation was prevented by cleaning the beaker thoroughly before each use.

The first fuel cell tested comprised of a nickel catalyst, nickel oxide plated with a palladium layer and phosphoric electrolyte. The gases used were oxygen and nitrogen instead of hydrogen. The fuel cell was tested to ensure that the gases flowed through and bubbles formed in the water to indicate that. However, when the testing machine was turned on and the temperature was increased, there was no current or voltage produced. This was thought to be caused by the nickel catalyst as platinum is usually used as the main catalyst in direct methanol and proton exchange membrane fuel cells. Thus, the next in the next fuel cell test the catalyst was changed to a carbon cloth with platinum. The fuel cell was tested again using the new catalyst and the current and voltage were measured at the same temperature range from room temperature to 200^0C. However, the fuel cell did not produce current or voltage. To determine if the cause was in the addition of palladium, the fuel cell was recreated using nickel oxide

without a palladium layer. It was ensured that gas diffusion layer (GDL) was catalyzed and a light layer of the phosphoric acid electrolyte was brushed on the carbon cloth with platinum catalyst.

The third test of the fuel cell used a NiO piece that did not have any plating. This was used to determine if the problems with current and voltage production were caused by the palladium layer. When tested, cell potential was finally produced as shown by Figure 18.

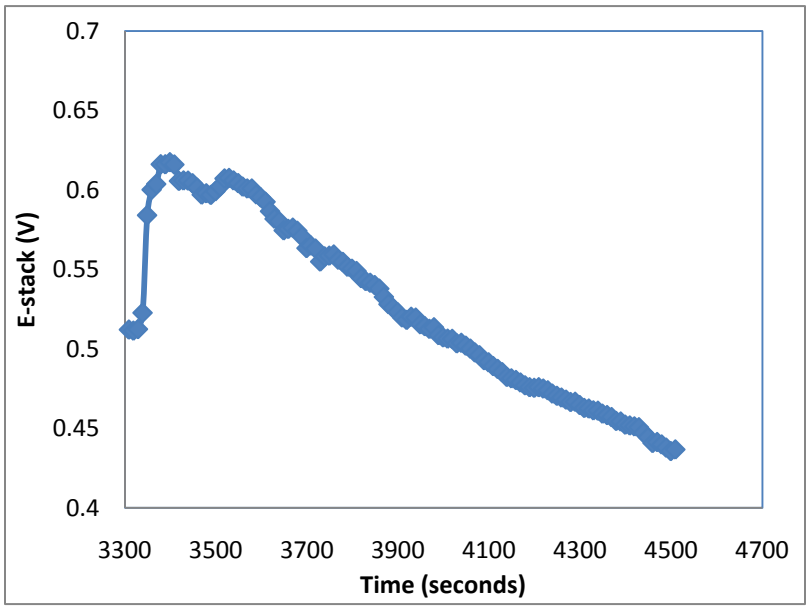

Figure 18: Experimental data, measured Cell Potential with a NiO membrane and phosphoric acid

Figure 18 illustrates the potential measured in the experiment. While the temperature rose from room temperature to approximately 80^0C, nitrogen fuel was used and data was not recorded. However, after switching to Oxygen and Hydrogen fuel, the data was recorded. The stack potential measured was approximately 0.7 but it decreased as time continued. This is similar to theoretical data when potential is plotted as a function of current. Overpotential causes the sharp decrease at first and then the rate slows down as current increases. As there was no current, the reason for the decrease in the potential was the transfer of the phosphoric acid from the NiO to the catalyst layer. The electrolyte layer thus dries and causes crossover and a decrease in OCV. There may be some resistance in the cell as well,

especially ohmic resistance, which causes the decrease in voltage. The initial increase in the potential occurred while the system leveled off and the program started running.

5. Conclusion and Recommendations

The fuel cell tests were conducted testing the use of palladium plated nickel oxide (NiO) membrane, phosphoric acid electrolyte and NiO without any plating as part of a direct methanol fuel cell operating at 150-200^{0}C. Electroless palladium plating of the NiO was proven a great method of depositing palladium to the surface. The layer thickness was controlled by the number of platings after determining the rate of plating. The palladium layer was also very dense. Experiments showed no diffusion of oxygen, nitrogen but only hydrogen, which is advantageous in reducing methanol crossover in DMFC. The maximum amount of phosphoric electrolyte soaked into the NiO was 0.5%, while the minimum was 0.027%. This may have caused the fuel cell to fail in producing any current or voltage. Thus, the method of depositing the electrolyte should be reevaluated. It may be advantageous to deposit the electrolyte in a different manner or to keep NiO soaked in the phosphoric acid at 100^{0}C for longer than 2.5 hours. Overnight soaking at that temperature should be investigated to determine if that produces optimum amount of electrolyte in NiO membrane.

More tests also need to be performed on the NiO plated with palladium to determine the reasons it does not work as theorized. According to other experiments conducted, electroless palladium plated nafion membranes were successful in producing current and voltage. Thus, the NiO should work theoretically. As mentioned before, the cause may have been the lack of electrolyte and increasing the amount of phosphoric acid may improve performance. Using molten potassium hydroxide as an electrolyte may also improve performance and should be investigated. Another recommendation is using methanol as a fuel in order to determine if the NiO support and phosphoric acid electrolyte are viable options in DMFC operation. This would increase the temperature range of DMFC's from room temperature and 80 degrees Celsius to 150-200 degrees Celsius.

References

Arico, A. S., S. Srinivasan and V. Antonucci. "DMFCs: From Fundamental Aspects to Technology Development." Fuel Cells (2001).

Bagotsky, Vladmir S. Fuel Cells: Problems and Solutions. Hoboken, NJ: John Wiley & Sons, Inc., 2009.

Choi, Won Choon, Ju Dam Kim and Seong Ihl Woo. "Modification of Proton Conducting Membrane for Reducing Methanol Crossover in a Direct-Methanol Fuel Cell." Journal of Power Sources 96 (2001): 411-414.

Cruickshank, John and Keith Scott. "The Degree and Effect of Methanol Crossover in the Direct Methanol Fuel cell." Journal of Power Sources 70 (1998): 40-47.

Datta, Ravindra. CHE 371X: Fuel cell Classnotes. Worcester, MA, 2010.

Garcia, Brenda L., et al. "Methanol Model of a Direct Methanol Fuel Cell." Journal of Fuel Cell Science and Technology (2004): 43-48.

Gleason, Denise A., Kristopher G. Jensen and Garima Painuly. Proton Exchange Membranes and Membrane Electrode Assemblies for Enhanced Direct Methanol Fuel Cell Performance. Major Qualifying Project. Worcester, MA, 2008.

Hai, Sun, et al. "Pd Electroless Plated nafion Membrane For High Concentration DMFCS." Journal of Membrane Science 259 (2005): 27-33.

Hamnett, A. "Mechanism and Electrocatalysis in the Direct Methanol Fuel Cell." Catalysis Today 38.4 (1997): 445-457.

Jorissen, L., et al. "New Membranes for Direct Methanol Fuel Cells." Journal of Power Sources 105 (2002): 267-273.

Jung, Doo Hwan, et al. "Performance of Direct Methanol Polymer Electrolyte Fuel Cell." Journal of Power Science 71 (1998): 169-173.

Larmine, James and Andrew Dicks. Fuel Cell Systems Explained, 2 Edition. England: John Wiley & Sons Ltd., 2003.

Liu, Hansan, et al. "A Review of Anode Catalysis in the Direct Methanol Fuel Cell." Journal of Power SOurces (2006): 95-110.

Mardilovich, Peter P., et al. "Defect-Free Palladium Membranes on Porous Stainless-Steel Support." AIChE (1998): 310-322.

Ramya, K and K.S. Dhathathreyan. "Direct Methanol Fuel Cells: Determination of Fuel Crossover in a Polymer Electrolyte Membrane." Journal of Electroanalytical Chemistry 542 (2003): 109-115.

Scott, K., W. Taama and J. Cruickchank. "Performance and Modelling of a Direct Methanol Solid Polymer Electrolyte Fuel Cell." Journal of Power Sources (1997): 159-171.

Spiegel, Colleen S. Designing & Building Fuel Cells. New York, NY: McGraw-Hill , 2007.

Sundmacher, K., et al. "Dynamics of the Direct Methanol Fuel Cell (DMFC): Experiments and Model-Based Analysis." Chemical Engineering Science 56 (2001): 333-341.

U.S. Department of Defense Fuel Cell Test and Evaluation Center (FCTec). "Direct Methanol Fuel Cells." 2010. FCTec. January 2010 <http://www.fctec.com/fctec_types_dmfc.asp>.

U.S. Department of Energy. Fuel Cell Technologies Program. 31 June 2009. November 2009 <http://www1.eere.energy.gov/hydrogenandfuelcells/fuelcells/fc_types.html>.

U.S. Energy Information Administration. U.S. Energy Information Administration. 2010. February 2010 <http://tonto.eia.doe.gov/energyexplained/index.cfm?page=us_energy_home>.

Wang, Z. H. and C. Y. Wang. "Mathematical Modeling of Liquid-Feed Direct Methanol Fuel Cells." Journal of Electrochemical Society (2003): A508-A519.

Yuming, Yang and Yung C. Liang. "Modeling and Analysis of a Direct Methanol Fuel Cell with Under-rib Mass Transport and Two-phase Flow at the Anode." Journal of Power Source. 194 (2009): 712-729.

Zhang, J. and Y. Wang. "Modeling the Effects of Methanol Crossover on the DMFC." Fuell Cells, Vol 4 (2004): 90-95.

Appendices

Appendix 1: Procedures for Membrane Treatment

Preparing NiO:

1. A 4 cm by 4 cm piece of nickel was first cleaned by sonicating it in a beaker of water for 15 minutes
2. It was then sonicated for 15 minutes in a beaker of acetone.
3. The nickel was then put in an oven, which was programmed to increase temperature from 30^0C to 990^0C at 5^0C per minute and then remain at 990^0C for 3 hours before cooling back at the same rate to 30^0C.

The recommended temperature for NiO treatment is 1100^0C but the oven used could not support such high temperatures, thus 990^0C was used.

Plating the NiO:

1. NiO was first placed in water for 5 minutes
2. Then 1 minute in 1M HCL solution
3. It was placed again in a water beaker while the rest of the beakers were filled with solutions
4. The sensitization of NiO was performed by placing it in a solution of $SnCl_2$ for 5 minutes.
5. It was then cleaned by placing it in a beaker of water labeled H_2O (1) for 2 minutes
6. This was followed by 3 minutes in beaker of water labeled H_2O (2)
7. The NiO was then activated by placing in a solution of $PdCl_2$ for 5 minutes
8. It was then placed in a solution of 0.01M HCL for 2 minutes
9. It was then placed in water for 3 minutes in a beaker labeled H_2O after 0.01M HCL
10. This process took 20 minutes from sensitization. It was repeated 4 times.
11. The activated NiO was then plated by first cleaning the piece in water for 5 minutes, followed by one minute in 1M HCL solution.
12. It was placed again in a water beaker while the rest of the plating solution was finalized.
13. The NiO was then placed in the plating solution and in a 60^0C bath for 90 minutes.
14. After 90 minutes, the solution was put in water while the plating solution was renewed. The water had been placed in the bath to remain at the same temperature as the plating solution.
15. The plating process was repeated 3 times to get a palladium layer of 5.1 µm.
16. The palladium plated NiO was then placed in a 120^0C for at least an hour and then stayed at 40^0C overnight while it dried.

The $SnCl_2$ solution must be prepared fresh each day it is used.

Before plating, approximately 70ml of the plating solution must be mixed with 1M H_2NNH_2

Preparations of Solutions:

1M HCL Solution:

- In a 1000ml beaker, add 250 ml water
- Add 100 ml 10M (concentrated, ~37%) HCL
- Fill the rest with water till 1000ml

0.01M HCL Solution:

- In a 1000ml beaker, add 250 ml water
- Add 1 ml 10M (concentrated, ~37%) HCL using syringe
- Fill the rest with water till 1000ml

$PdCl_2$ Solution:

- In a 1000ml beaker, add 250 ml water
- Add 1 ml 10M (concentrated, ~37%) HCL using syringe
- Add 0.1g $PdCl_2$
- Put solution on a stirrer on low and turned heater to approximately 60^0C for an hour.
- Fill the rest with water till 1000ml

Plating Solution:

- In a 1000ml beaker, add 250 ml water
- Add 198 ml NH_4OH
- Add 4 g of $Pd(NH_3)_4Cl_2$ and shake gently to dissolve
- Add 40.1 g of Na_2EDTA and shake gently to dissolve
- Fill the rest with water till 1000ml

$SnCl_2$ Solution:

- In a 1000ml beaker, add 250 ml water
- Add 1 ml 10M (concentrated, ~37%) HCL using syringe
- Add 1g $SnCl_2$ $2H_2O$ and shake gently to dissolve
- Put solution on a stirrer on low and turned heater to approximately 60^0C for an hour.
- Fill the rest with water till 1000ml

1M H_2NNH_2:

- In a 25ml beaker, add 10 ml water
- Add 0.8 ml 1M H_2NNH_2 using syringe
- Fill the rest with water till 25ml

Calculating the thickness of the palladium layer

The palladium layer thickness was calculated as follows:

$$Thickness\ of\ Palladium = \frac{The\ change\ in\ weight\ of\ the\ NiO\ (g) * 1000}{density\ of\ Palladium * surface\ area\ of\ plated\ part}$$

The density of palladium is 12mg/cm^3.

For example,:

The initial weight of NiO before plating was 1.1052g and the final weight after plating was 1.15g. The surface area was calculated to be 3.211 cm^2. Thus the Pd thickness was:

$$Thickness\ of\ Palladium = \frac{0.0448\text{g} * 1000}{\frac{12mg}{cm^3} * 3.211\ cm^2} = 12.46\mu m$$

The rate of plating is determined by dividing the thickness of the palladium by the number of hours plated.

This for the above example, the rate would be:

$$Rate\ of\ plating = \frac{12.46}{4\ platings * 90\frac{minutes}{plating}} = \frac{2.07\mu m}{hour}$$

Calculating the amount of phosphoric acid impregnated in the NiO

To determine the amount of phosphoric acid in the NiO, the change in weight of the NiO was divided by the original weight.

$$\%\ Phosphoric\ acid\ impregnated = \frac{The\ change\ in\ weight\ of\ the\ NiO\ (g) * 100}{Initial\ weight\ of\ NiO}$$

Appendix 2: Thermodynamic Functions Calculations

Table 4: Parameters for anode (A), cathode (C), and overall reaction (OR) thermodynamics

I	$G^{o}_{f,I}$ (J/mol)	$H^{o}_{f,I}$ (J/mol)
CH_3OH	-162600	-201300
H_2O	-237140	-285830
CO_2	-394390	-393510
H^+	0	0
e^-	0	0
O_2	0	0

The change in Gibbs Free energy when potential is zero is calculated by adding the Gibbs free energies of formation each multiplied by the stoichiometric coefficients of the species as follows using the information in table 1.

$$\Delta G^0_{A,\varphi=0} = G^0_{f,CO_2} + 6G^0_{f,H^+} + 6G^0_{f,e^-} + (-1)G^0_{f,CH_3OH} + (-1)G^0_{f,H_2O}$$

$$\Delta G^0_{C,\varphi=0} = 3G^0_{f,H_2O} + \left(-\frac{3}{2}\right)G^0_{f,O_2} + (-6)G^0_{f,H^+} + (-6)G^0_{f,e^-}$$

$$\Delta G^0_{OR,\varphi=0} = G^0_{f,CO_2} + 2G^0_{f,H_2O} + (-1)G^0_{f,CH_3OH} + \left(-\frac{3}{2}\right)G^0_{f,O_2}$$

The change in enthalpy is calculated by a similar method using the information in table 1.

$$\Delta H^0_A = H^0_{f,CO_2} + 6H^0_{f,H^+} + 6H^0_{f,e^-} + (-1)H^0_{f,CH_3OH} + (-1)H^0_{f,H_2O}$$

$$\Delta H^0_C = H^0_{f,H_2O} + \left(-\frac{1}{2}\right)H^0_{f,O_2} + (-2)H^0_{f,H^+} + (-2)H^0_{f,e^-}$$

$$\Delta H^0_{OR} = H^0_{f,CO_2} + 2H^0_{f,H_2O} + (-1)H^0_{f,CH_3OH} + \left(-\frac{3}{2}\right)H^0_{f,O_2}$$

The change in entropy is calculated by dividing the difference between enthalpy change and Gibbs free energy change by standard temperature, which is 298K.

$$\Delta S^0_\rho = \frac{\Delta H^0_\rho - \Delta G^0_{\rho,\varphi=0}}{298\ K}, \qquad \rho = A, C, OR$$

The standard equilibrium is calculated as shown:

$$\Phi_{0,\rho}^{0} = \frac{\Delta G_{\rho,\varphi=0}^{0}}{v_{\rho e^-} F}, \qquad \rho = A, C$$

The results of the calculations for the thermodynamic functions are as follows in table 2.

Table 5: Standard thermodynamic functions and electrode potentials

P	$\Delta G_{p,\Phi=0}^{0}$ (J/mol)	ΔH_p^0 (J/mol)	ΔS_p^0 (J/mol*K)	$\Phi_{0,p}^{0}$ (V)
Anode	5350	93620	296	$9.24*10^{-3}$
Cathode	-711420	-857490	-490	1.229
Overall Reaction (OR)	-706070	-763870	-193.96	

Appendix 3: Reversible Efficiency

To determine the reversible efficiency, the standard equilibrium cell potential and standard maximum voltage are calculated as follows:

$$\mathrm{V}_0^0 = \frac{-\Delta G_{OR,\varphi=0}^0}{n_e - F} \; or \; \mathrm{V}_0^0 = \; \Phi_{0,C}^o - \; \Phi_{0,A}^o = 1.21976\, V$$

$$\mathrm{V}_{Max}^0 = \frac{-\Delta H_{OR}^0}{n_e - F} = 1.319\, V$$

The reversible efficiency was then given by:

$$\varepsilon_0 = \frac{V_0}{V_{Max}} = \frac{\mathrm{V}_0^0}{\mathrm{V}_{Max}^0} - \; (T - T^0)\left(\frac{\Delta S_{OR}^0}{\Delta_{OR}^0}\right) = \; 0.910367228$$

Where T=353K and T^0=298K

Appendix 4: Feasibility Curves Calculations

The Nerst Equation was used to determine the parameters for the feasibility curves as shown:

$$K_{p,\Phi=0} = \exp\left(\frac{\Delta S_p^0}{R}\right) * \exp\left(-\frac{\Delta H_p^0}{RT}\right)$$

$$K_p = K_{p,\Phi=0} * \exp\left(\frac{\nu_{pe^-} F * \Phi}{RT}\right) = \exp\left(\frac{\Delta S_p^0}{R}\right) * \exp\left(-\frac{\Delta H_p^0}{RT}\right) * \exp\left(\frac{\nu_{pe^-} F * \Phi}{RT}\right)$$

$$In\ K_p = \left(\frac{\Delta S_p^0}{R}\right) - \left(\frac{\Delta H_p^0}{RT}\right) + \frac{\nu_{pe^-} F * \Phi}{RT}$$

K_p was set to zero to solve for T:

$$T = \frac{-\Delta H_f + (\nu_{pe^-} * F * \phi)}{\Delta S_0^0}$$

The parameters for the feasibility curves were calculated for when T=0 and Φ=0

Table 6: Parameters for feasibility curves

Anode		Cathode	
T(K)	Φ (V)	T(K)	Φ (V)
0	0.000162	0	1.481184
316.2838	0	1749.98	0

Appendix 5: MathCAD Calculations for the electrode potentials

If Solving for Electrode Potential (V)

$iao := 1.414$ $ico := 0.00063$ $aa := 0.5$ $ac := 0.5$

$E := 6$ $f := 9648$ $ix := 0.$ $t := 353$

$i := 0.$ $ial := 41.$ $ixc := i$ $icl := 0.$

guess

$v := 0.1$

Anode $Ec := -2$

Given

$$\exp\left(\frac{aa \cdot E \cdot f \cdot v}{r \cdot t}\right) - \exp\left[\frac{[(aa - 1) \cdot E \cdot f \cdot v]}{r \cdot t}\right] = \frac{(i + ix)}{iao \left(1 - \frac{(i+ix)}{ial}\right)}$$

$$Find(v) = 2.748 \times 10^{-3}$$

Cathode

$icl := 0.$

Given

$$\exp\left[\frac{(ac \cdot Ec \cdot f \cdot v)}{r \cdot t}\right] - \exp\left[\frac{[(ac - 1) \cdot Ec \cdot f \cdot v]}{r \cdot t}\right] = \frac{(i + ixc)}{ico \left(1 - \frac{(i+ixc)}{icl}\right)}$$

$$Find(v) = 0.217$$

Appendix 6: Raw Data

Raw data from the calculations of Power, Efficiency, Voltage, Cathode and Anode Potential

i	V	n_A	n_C	P	ε
0	0.898493	0.001507	0	0	0.681193
0.1	0.715964	0.001873	0.172	0.071596	0.542808
0.2	0.67644	2.24E-03	0.201	0.135288	0.512843
0.3	0.647921	2.59E-03	0.219	0.194376	0.491222
0.4	0.623408	2.94E-03	0.233	0.249363	0.472637
0.5	0.601899	3.29E-03	0.244	0.300949	0.45633
0.6	0.582397	3.63E-03	0.253	0.349438	0.441545
0.7	0.563901	3.96E-03	0.261	0.394731	0.427521
0.8	0.54641	4.29E-03	0.268	0.437128	0.414261
0.9	0.528926	4.61E-03	0.275	0.476033	0.401005
1	0.512447	4.93E-03	0.281	0.512447	0.388512
1.1	0.496974	5.24E-03	0.286	0.546672	0.376781
1.2	0.481509	5.54E-03	0.291	0.577811	0.365056
1.4	0.451595	6.13E-03	0.3	0.632232	0.342376
1.6	0	6.30E-03	0.308	0	0